European Heart Journal (2010) **31**, 401–415
doi:10.1093/eurheartj/ehp433

REVIEW

Imaging of atherosclerosis: optical coherence tomography (OCT)

Expert review document on methodology, terminology, and clinical applications of optical coherence tomography: physical principles, methodology of image acquisition, and clinical application for assessment of coronary arteries and atherosclerosis

Francesco Prati[1]*, Evelyn Regar[2], Gary S. Mintz[3], Eloisa Arbustini[4], Carlo Di Mario[5], Ik-Kyung Jang[6], Takashi Akasaka[7], Marco Costa[8], Giulio Guagliumi[9], Eberhard Grube[10], Yukio Ozaki[11], Fausto Pinto[12], and Patrick W.J. Serruys[2] for the Expert's OCT Review Document

[1]Interventional Cardiology, San Giovanni Hospital, Via dell'Amba Aradam, 8, 00184 Rome, Italy; [2]Thoraxcenter, University Hospital Rotterdam, Rotterdam, the Netherlands; [3]Washington Hospital Center, Washington, DC, USA; [4]IRCCS Foundation Policlinico San Matteo, Pavia, Italy; [5]Royal Brompton Hospital and Imperial College, London, UK; [6]Massachusetts General Hospital, Boston, MA, USA; [7]Wakayama Medical University, Wakayama, Japan; [8]Medical Center Cleveland, Cleveland, OH, USA; [9]Spedali Riuniti, Bergamo, Italy; [10]Heart Center Siegburg, Siegburg, Germany; [11]Fujita Health University, Fujita, Japan; and [12]University of Lisbon, Lisbon, Portugal

Received 10 December 2008; revised 30 April 2009; accepted 12 June 2009; online publish-ahead-of-print 4 November 2009

Optical coherence tomography (OCT) is a novel intravascular imaging modality, based on infrared light emission, that enables a high resolution arterial wall imaging, in the range of 10–20 microns. This feature of OCT allows the visualization of specific components of the atherosclerotic plaques. The aim of the present Expert Review Document is to address the methodology, terminology and clinical applications of OCT for qualitative and quantitative assessment of coronary arteries and atherosclerosis.

Keywords Atherosclerosis • OCT • Intravascular imaging • Angioplasty

Introduction

This document represents a review of the fundamental concepts and current clinical applications of intravascular optical coherence tomography (OCT). The goal is to provide a framework for standardization of terminology for the appropriate use and report of OCT imaging. While this is not a clinical guideline document, the expressed opinions represent a consensus among clinicians and investigators with a large experience in the utilization and evaluation of OCT technology. The document focuses on the physical principles, methodology of image acquisition, and clinical diagnostic applications.

Physical principles and technique for optical coherence tomography imaging

Optical coherence tomography is an imaging modality that is analogous to ultrasound imaging, but uses light instead of sound. Cross-sectional images are generated by measuring the echo time delay and intensity of light that is reflected or back-scattered from internal structures in tissue.[1–5] Optical coherence tomography improves localization of the returned signal origin due to the much shorter wavelength of the imaging light when compared

* Corresponding author. Tel: +39 06 77 05 53 30, Email: fprati@hsangiovanni.roma.it

Table 1 Physical characteristics of optical coherence tomography vs. IVUS

	OCT[a]	IVUS[b]
Energy source	Near-infrared light	Ultrasound (20–45 MHz)
Wave-length, μm	1.3	35–80
Resolution, μm	15–20 (axial); 20–40 (lateral)	100–200 (axial); 200–300 (lateral)
Frame rate, frames/s	15–20	30
Pull-back rate, mm/s	1–3	0.5–1
Max. scan diameter, mm	7	15
Tissue penetration, mm	1–2.5	10

OCT, optical coherence tomography.
[a]Based on specification of the LightLab M2/M3 time domain OCT imaging system.
[b]Based on specifications of the current generations of Volcano, Boston Scientific, and Terumo IVUS systems.

with ultrasound; hence, OCT offers significantly improved resolution. As the speed of light does not allow direct measurement of the echo time delay, interferometric techniques have been developed to analyse the reflected light signal.

There are two main technologies that can be used to obtain OCT images: time domain and frequency domain. Frequency domain OCT has the advantage of an improved signal-to-noise ratio allowing extremely fast-scanning laser systems to increase imaging speed while delivering comparable or improved image quality vs. the earlier time domain systems. It is worth noting that basic OCT characteristics do not change when moving from time domain to frequency domain OCT. Frequency domain OCT is in an advanced stage of development but is still non-available for commercial use. Therefore in the present paragraph and overall text we refer to time domain OCT obtained with the Light Lab (Light Lab Imaging, USA) technology since this is the only one that is commercially available.

However, some of the current statements and recommendations may change when future technical solutions based on frequency domain technology become available. As the OCT beam can be delivered via thin submicrometrics fibre optics, ultraminiaturized intravascular catheters and wires can be developed to image coronary arteries. Commercially available OCT catheters or wires have a single mode optical fibre encased in a hollow rotating torque cable coupled to a distal lens and a microprism that directs the OCT beam, orthogonally outward from the catheter. The cable and the distal optics are encased in a transparent housing.

Current OCT images are obtained at a peak wavelength in the 1280–1350 nm band that enables a 10–15 μm tissue axial resolution, 94 μm lateral resolution at 3 mm, and maximal scan diameter of 6.8 mm. Images are then displayed using a log false colour scale, at 20 frames per second and 200 lines per frame. These variables are expected to improve considerably with the new frequency domain systems. Time domain OCT physical characteristics are shown and compared with IVUS in *Table 1*. Resolution is determined by the intrinsic wavelength range (bandwidth) of the light source utilized; the detection efficiency or signal-to-noise ratio determines the feasible image acquisition speed, and tissue scattering and absorption properties determine the tomographic penetration depth and the contrast and brightness of the OCT image. Recent technological advances have seen acquisition speeds improve dramatically[6–9] and resolution has been steadily improving in clinical systems from approximately 15–20 μm axially to 10 μm or better (research systems have shown resolutions <5 μm). The penetration depth of OCT imaging is limited almost entirely by basic tissue optical properties and remains the chief limitation of the technique providing between 0.5 and 1.5 mm of imaging depth in most tissue types, with no foreseeable possibilities of future technical improvement. As a second limitation OCT cannot image through a blood field necessitating clearing or flushing blood from the lumen. In addition, at the current stage of technology, measurement of large-diameter vessels at proximal target sites can pose difficulties for OCT in the clinical setting, particularly for the measurement of ostial lesions in the left main and right coronary arteries.

Optical coherence tomography image acquisition

The main obstacle to the adoption of OCT imaging in clinical practice is that OCT cannot image through a blood field, as it requires clearing or flushing blood from the lumen. Insufficient blood clearance during image acquisition can greatly deteriorate the quality of the images. Most of the earliest published OCT studies were performed with an OCT catheter derived from a modified IVUS design.[10] The pioneering work of Jang *et al.*[11] involved clearing of the blood from the field of view during intermittent 8–10 ml saline flushes through the guiding catheter. This technique allowed only a brief visualization of the target lesion, but this no longer applies to the two automated techniques of OCT acquisition that are currently used.

The occlusive technique. During imaging acquisition, coronary blood flow is stopped by inflating a proximal occlusion balloon and flushing a crystalloid solution, usually Ringer's lactate, through the end-hole of the balloon catheter at a flow rate of 0.5–1.0 mL/s. The vessel occlusion time should be adjusted according to patient symptoms and severity of ECG changes (QRS duration and QT prolongation) with infusion set to stop automatically after a maximum of 35 s to avoid haemodynamic instability or arrhythmias.[12,13] A power injector is recommended for injection of the flush solution at a constant rate. Multiple pull-

backs can be performed to accomplish complete lesion assessment. Three limitations to this technique are: (i) inadequate clearing of the lumen affecting image clarity because of balloon-vessel size mismatch (the balloon is too small to occlude the vessel) or backward blood flow from well-developed collaterals; (ii) scanning through a long diseased lesion when the length of the lesion exceeds 30 mm,[5] and (iii) the fact that ostial or very proximal lesions (<15 mm from ostium) are not suitable for imaging.

Non-occlusive technique. The non-occlusive mode of acquisition, recently developed and not yet supported by the manufacture, does not require proximal balloon occlusion. A standard intracoronary guide wire is generally used to cross the target lesion and to enable insertion of an over-the-wire intracoronary probe with an inner lumen compatible with the diameter of the OCT probe (0.019 in.). The guide wire is then switched with the Light Lab ImageWire and pull-back is performed at the highest available speed during simultaneous infusion of a viscous iso-osmolar solution through the guiding catheter.

One infusion protocol requires manual injection of a commercially available contrast agent (Iodixanol 320, Visipaque™, GE Health Care, Ireland) through the guiding catheter at an infusion rate between 1 and 3 ml/s, based on the run-off of the artery and the online assessment of OCT image quality. This contrast agent is recommended both for its low arrhythmogenic potential and for its high viscosity, helpful to prolong imaging time. Large series show that the blood can be completely displaced from the artery during the entire acquisition period.[14,15] Technical developments described below have the potential to drastically reduce the imaging time so that a very short hand- or power-injection will suffice for optimal image acquisition.

Due to its ease and safety, the OCT non-occlusive technique is an alternative approach favoured by some.

Safety of optical coherence tomography

The applied energies in intravascular OCT are relatively low (output power in the range of 5.0–8.0 mW) and do not cause functional or structural damage to the tissue. The safety of OCT thus depends mainly on the mechanical characteristics of the catheter and the extent of ischaemia caused by flow obstruction from the occlusion balloon or the amount of contrast injected when the non-occlusive technique is employed.

Preliminary experiences with both occlusive and non-occlusive OCT images acquisition show the technique to be safe. Optical coherence tomography imaging technique has gained considerable adoption in many centres across Europe and Japan, and various centres have presented large series of patients imaged by OCT without major complications. The technology is not approved yet in the United States.

There are two reports on the safety of intracoronary OCT imaging. No major complications or arrhythmias were reported in a preliminary study of 60 patients studied using the non-occlusive technique even though a large number of these patients had acute coronary syndrome. One patient had a rise in CK-MB enzymes, likely a consequence of the percutaneous coronary intervention, rather than the OCT study. Ischaemic ECG changes were transient and occurred in 21 patients (35%), with ST depression in 17 (28.3%) and ST elevation in 4 (6.7%). Seven patients (11.7%) had angina. Ventricular ectopic beats were found in six patients (10%); other major arrhythmias (ventricular tachycardia of fibrillation) were not observed. All electrocardiographic signs and patient's symptoms rapidly resolved at the completion of the image acquisition procedure.[15]

Preliminary data also supports the safety of the occlusive OCT image acquisition technique. A multicentre study reported on the safety of the occlusive acquisition technique in 76 patients with coronary artery disease. Vessel occlusion time averaged 48.3 ± 13.5 s; and no major complications such as myocardial infarction, emergency revascularization, or death occurred. Also, there were no significant procedural complications including ventricular tachycardia or ventricular fibrillation, acute vessel occlusion, dissection, thrombus formation, embolism, or vasospasm.[16] No impairment in renal function or rise in serum creatinine up to 48 h after the procedure was observed.

Feasibility and effectiveness of optical coherence tomography imaging

Based on published data on the non-occlusive technique in 64 patients referred for coronary angioplasty, it was found that OCT was successful in 93.7%, with a mean amount of contrast given for the basal OCT assessment of 30.5 ± 3.3 mL (range 22–35 mL).[15] Data on OCT reproducibility showed two serial pull-backs to provide accurate measurement of luminal area with a high correlation for reproducibility (R 0.96, $P < 0.001$). Optical coherence tomography provides superior visualization and differentiation of the lumen and arterial wall interface when compared with IVUS; this facilitates determination of lumen areas and volumes. Also, in over 2000 analysed cross-sections, a high percentage (96%) showed good image quality with the whole circumference being well depicted.[14]

In the most comprehensive study of the occlusive technique to date, a 100% imaging success rate was observed.[16] Based on these encouraging preliminary findings, regardless the applied acquisition technique, an OCT study should be considered successful if at least 90% of the image cross-sections are of good quality.

In a comparative study between OCT (obtained with the occlusive technique) and IVUS, both led to a high procedural success. Also, OCT imaging wires, due to a low crossing profile were able to negotiate some tight lesions that the IVUS catheter was unable to cross.[16] There was a high correlation between measurements of lumen diameter and lumen area obtained with OCT and IVUS, although OCT measurements were found to be 7% smaller (5.2 ± 2.8 vs. 5.6 ± 2.6 mm^2, $P < 0.0001$).[16] The findings of smaller lumen sizes with OCT compared with IVUS may be related to several factors. The IVUS catheter itself may stretch small arteries (Dotter effect) because of its large size to produce artificial large vessel sizes; thus, differences between OCT and IVUS measurements may be more relevant in small vessels. Another possibility is that intracoronary perfusion pressure is reduced during balloon inflation to generate artificial smaller

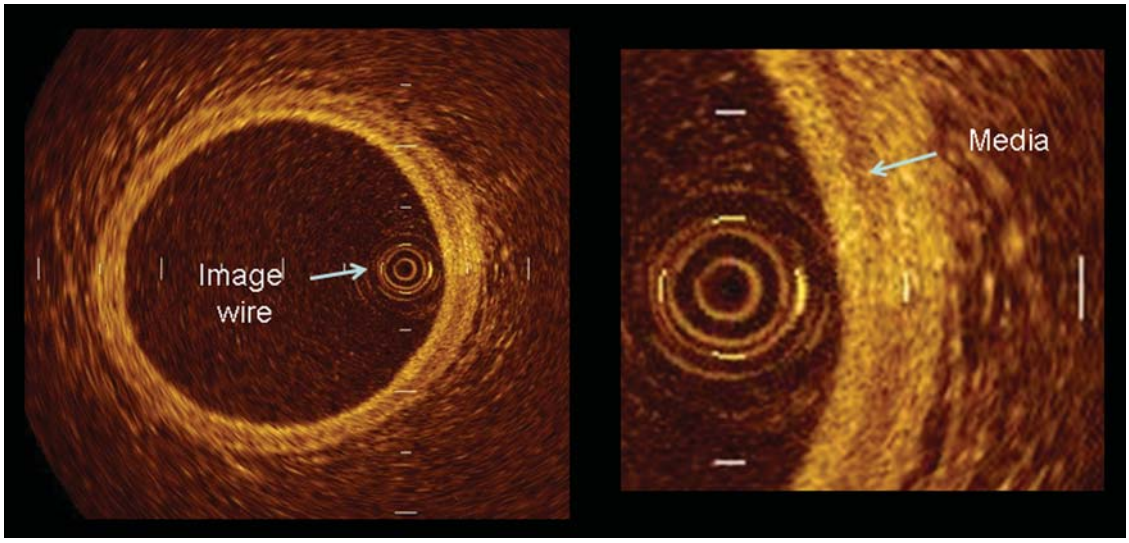

Figure 1 Optical coherence tomography shows the three layer appearance of normal vessel wall, with the muscular media being revealed as a low signal layer comprised between internal and external lamina.

vessel dimensions during OCT image acquisition. Lastly, this discrepancy may be due to the greater resolution of OCT, which enables an optimal definition of the lumen–plaque border. Optical coherence tomography has the potential to become the most accurate imaging modality to assess lumen dimensions and facilitate the application of automatic algorithms of measurements. However, further studies are needed to address both this point and the identification of lumen area values that discriminate lesions capable of inducing effort ischaemia.

However, IVUS still remains the most widely used and validated clinical intravascular imaging technique.

Normal coronary morphology

In normal vessels and at the sites of thin plaques, with thicknesses not exceeding 1.2 mm, the coronary artery wall appears as a three-layer structure in OCT images. The medium is seen as a dark band delimited by the internal elastic lamina (IEL) and external elastic lamina (EEL). Histologically, the IEL is constituted of a thin layer of elastic fibres (<3 μm). Despite its minimal thickness, the IEL generates a signal-rich band (around 20 μm) between the intima and media that is likely due not only to the IEL itself, but also to the gradient generated by the different tissue composition of the tunica media and intima. The EEL is constituted of a few, often discontinuous layers of short elastic fibres that span a thickness of 3–6 μm. Presence of the EEL causes a signal-rich band (around 20 μm) between the media and adventitia. The adventitia is a signal-rich, heterogeneously texted outer layer.

As the thickness of the media ranges from 125 to 350 μm (mean 200 μm), it can be visualized easily by OCT resolution[17,18] (*Figure 1*). In the presence of atherosclerosis, the media typically becomes thinner in the quadrants of plaque accumulation as a result of asymmetric expansion of the vessel wall during vessel remodelling. Because of its limited tissue penetration (1–1.5 mm), OCT does not appear to be suited to study vessel remodelling, which is well addressed by IVUS. In fact, in the presence of a large plaque burden, OCT does not penetrate sufficiently to allow visualization of the media.

The assessment of a normal intima is beyond the resolution of OCT because its thickness is only approximately 4 μm; this corresponds to a small sub-endothelial collagen layering and a single layer of endothelial cells that in normal vessels of children and youths are flattened. Intimal thickness, however, increases with age; nearly all coronary arteries of adults show some grade of intimal thickness; and a diffuse thickening of intima is a rather common process in advanced age and is histologically distinct from atherosclerosis. Because of its much higher resolution compared with IVUS,[19,20] OCT detects even the earliest stages of intimal thickening, depicted as a bright, homogeneous thin rim of tissue having a texture similar to fibrous plaque components (*Figure 2*). However, the identification of pathologic neointimal growth is limited by the lack of an established cut-off value.

Areas of consensus in assessment of atherosclerosis

Qualitative descriptions of atherosclerosis

Table 2 summarizes the appearance of atherosclerotic components by OCT and IVUS.

Calcifications within plaques are identified by the presence of well-delineated, low back-scattering heterogeneous regions[10,11,21–23] (*Figure 3*). Superficial micro-calcifications, considered to be a distinctive feature of plaque vulnerability, are revealed as small superficial calcific deposits. *Fibrous plaques* consist of homogeneous high back-scattering areas[10,11,21–23]

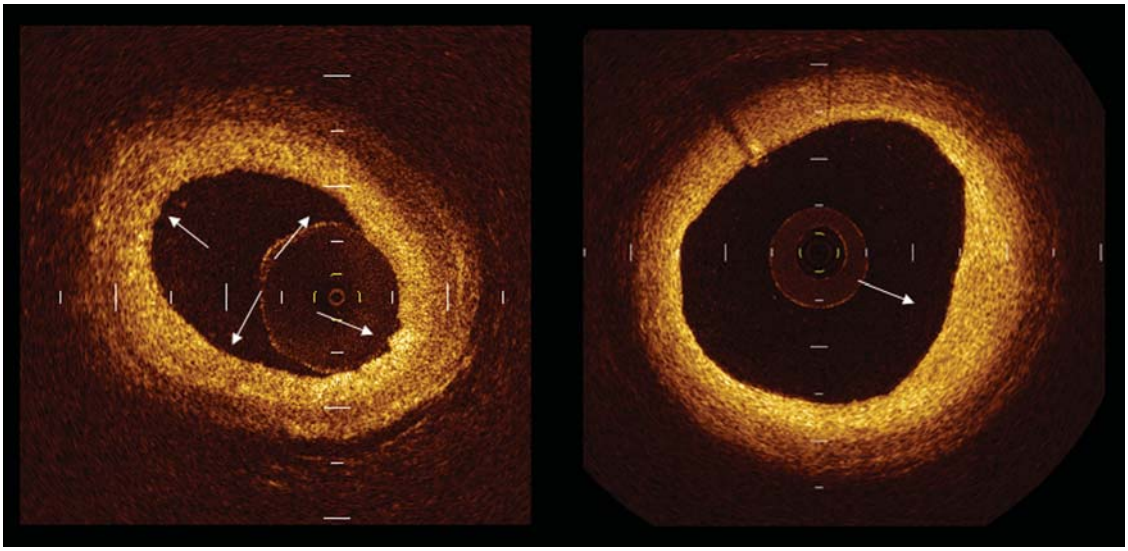

Figure 2 Example of intimal thickening revealed by optical coherence tomography as a bright homogeneous layer. The left panel shows a diffuse intimal thickening, the right panel a localized one (arrow).

Table 2 Image characteristics of optical coherence tomography vs. IVUS

Tissue type	Image characteristics	
	OCT	IVUS
Fibre	Homogeneous High reflectivity Low attenuation	Homogeneous High reflectivity
Calcium	Sharp edges Low reflectivity Low attenuation	Very high reflectivity Shadowing
Lipid	Diffuse edges High reflectivity High attenuation	Low backscatter
Red thrombus	Medium reflectivity High attenuation	Medium-high reflectivity
White thrombus	Medium reflectivity Low attenuation	

OCT, optical coherence tomography.

(*Figure 3*). *Necrotic lipid pools* are less well-delineated than calcifications and exhibit lower signal density and more heterogeneous back-scattering than fibrous plaques. There is a strong contrast between lipid-rich cores and fibrous regions within OCT images. Therefore, lipid pools most often appear as diffusely bordered, signal-poor regions (lipid pools) with overlying signal-rich bands, corresponding to fibrous caps[10,11,21–24] (*Figure 3*).

Thrombi are identified as masses protruding into the vessel lumen discontinuous from the surface of the vessel wall. Red thrombi consist mainly of red blood cells; relevant OCT images are characterized as high-backscattering protrusions with signal-free shadowing. White thrombi consist mainly of platelets and white blood cells and are characterized by a signal-rich, low-backscattering billowing projections protruding into the lumen[25] (*Figures 3* and *4*). In reality, pure white or red thrombi are rarely found; mixed thrombi, on the other hand, are common.

Despite the high resolution of OCT, in some circumstances non-protruding red thrombi can be misinterpreted for necrotic lipid pools. This may occur due to the similar OCT signal pattern of the two plaque components.[26]

Thrombi are frequently found within *culprit lesions* of patients with *acute coronary syndromes*.[15,21] A fresh or large thrombus may hamper the visualization of plaque features such as ulceration beneath the thrombus itself. To solve this problem when evidence of thrombosis is present, OCT cross-sections acquired within the coronary segment with thrombus should be searched one by one for sites where vessel wall and plaque morphology can be seen. In the presence of thrombosis, *three distinct OCT morphologies can be detected*: (i) either massive thrombosis or any amount of red thrombus that does not permit assessment of vessel and plaque morphology; (ii) thrombosis with signs of ulceration underneath, or (iii) thrombosis with apparently normal endothelial lining underneath that may be indicative of erosion. However, a firm diagnosis of erosion cannot be made without knowledge of the morphological or functional alterations of a single endothelial layer that cannot be assessed directly with OCT (*Figures 3–6*).

Plaque Dissections are common findings associated with ruptured plaques visualized by OCT. They are identified as rims of tissue protruding into the lumen[15] (*Figure 5*).

Acute plaque ulceration or rupture can be detected by OCT as a ruptured fibrous cup that connects the lumen with the lipid pool. These ulcerated or ruptured plaques may occur with or

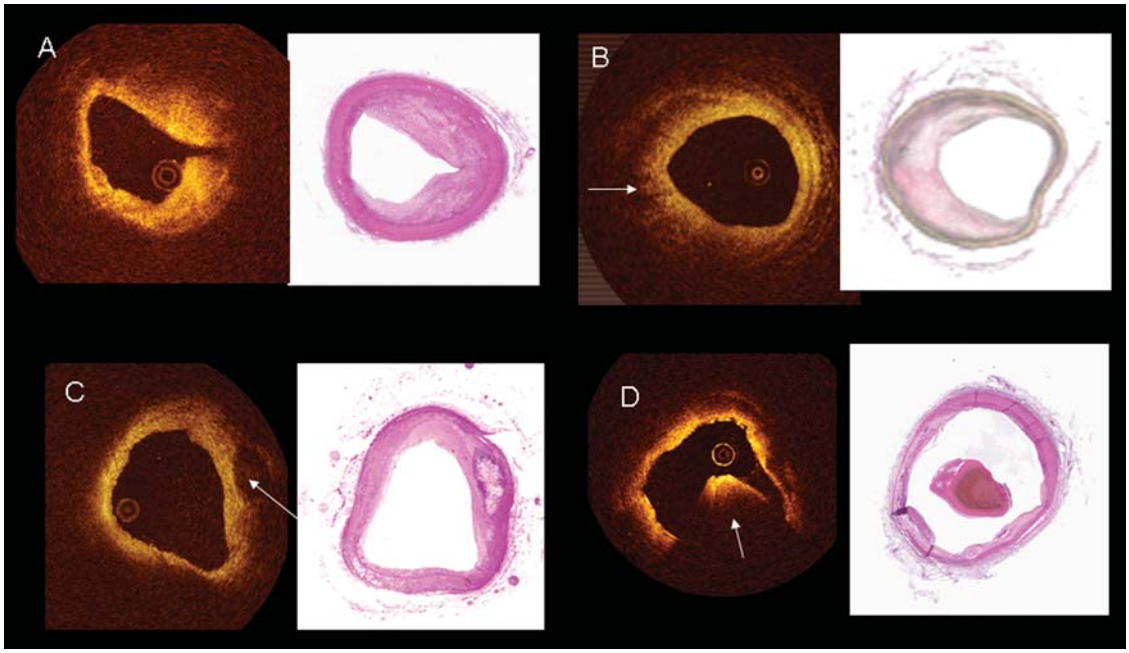

Figure 3 Optical coherence tomography examples of plaque composition (left panels) and corresponding histology (right panel). Diffusely fibrotic plaque (*A*), lipid pool (arrow in *B*), calcific component (arrow in *C*), and thrombus (arrow in *D*).

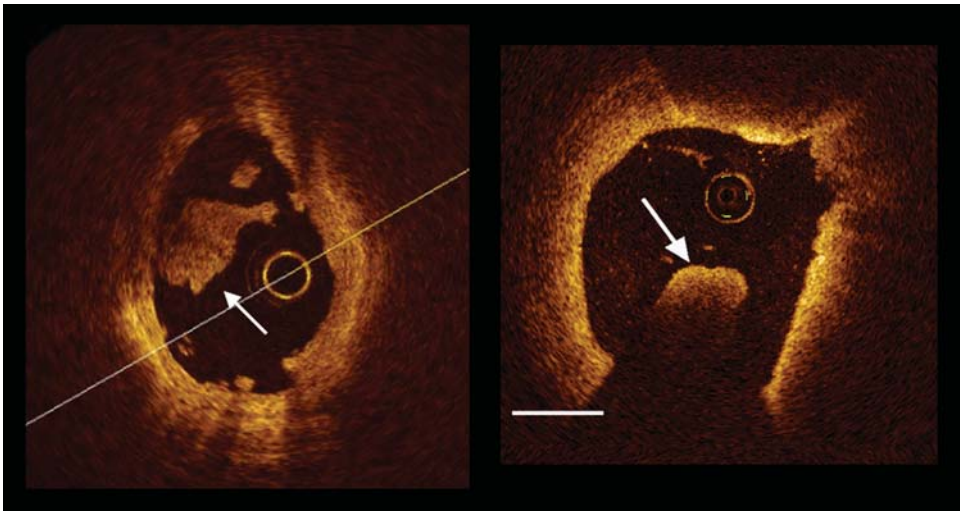

Figure 4 Example of white and red thrombus. White thrombus is platelet rich and exhibits a low signal attenuation (arrow in the left panel), while red thrombus, due to presence of red blood cells components, causes a marked signal attenuation (arrow in the right panel).

without a superimposed thrombus. When signs of ulceration are present without evidence of thrombosis, the lesion cannot be defined as a 'culprit' with certainty, unless clinical criteria provide some evidence that the lesion is responsible for the acute events. Use of thrombolysis, IIb–IIIa GP inhibitors, or other anti-thrombotic drugs facilitate clot degradation and in some circumstances may lead to complete disappearance (*Figures 6* and *7*).

It has to be stressed that identification of atherosclerotic plaque components by OCT depends on the penetration depth of the incident light beam into the vessel wall. The depth of penetration is greatest for fibrous tissue and least for thrombi with calcium and lipid tissue having intermediate values (*Figure 8*).

Additional clinical–pathological correlation studies, particularly with the new upcoming technologies, are important to further define tissue characteristics by OCT.

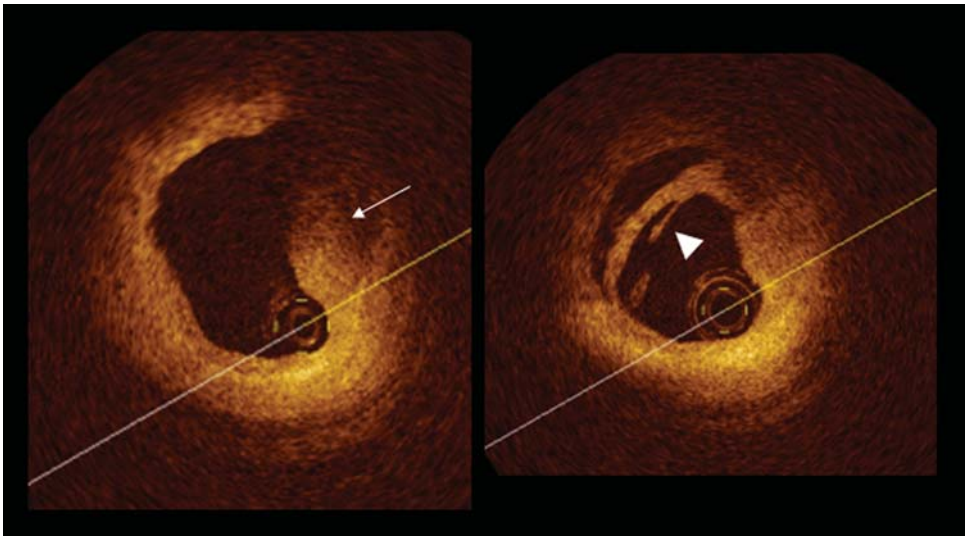

Figure 5 Atherosclerotic plaque with superficial lipid pool located at 1–3 o'clock (left panel). The right panel shows the plaque rupture at the site of plaque shoulder, with a clear rim of dissection (arrow head).

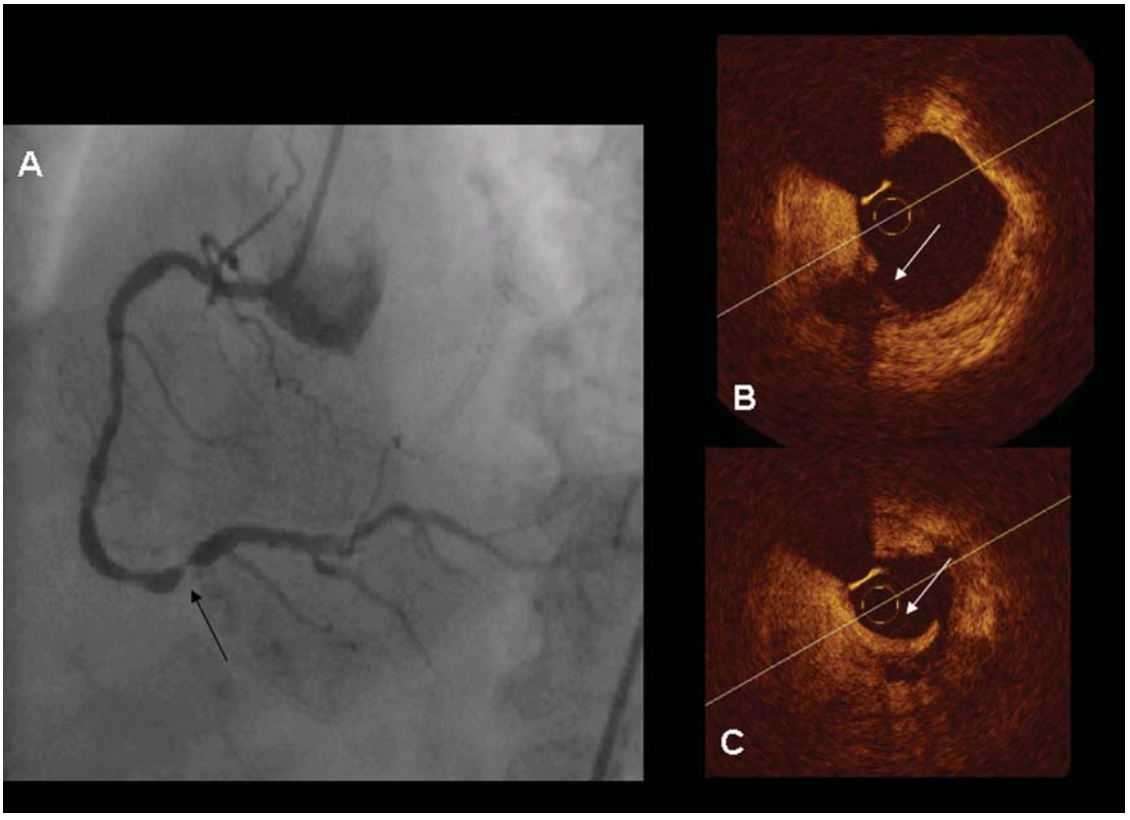

Figure 6 Example of culprit lesion in the right coronary artery (arrow in *A*). (*B*) shows a superficial ruptured lipid pool (arrow), while (*C*) reveals an intracoronary thrombosis (arrow). Arrowheads indicate image wire artefacts.

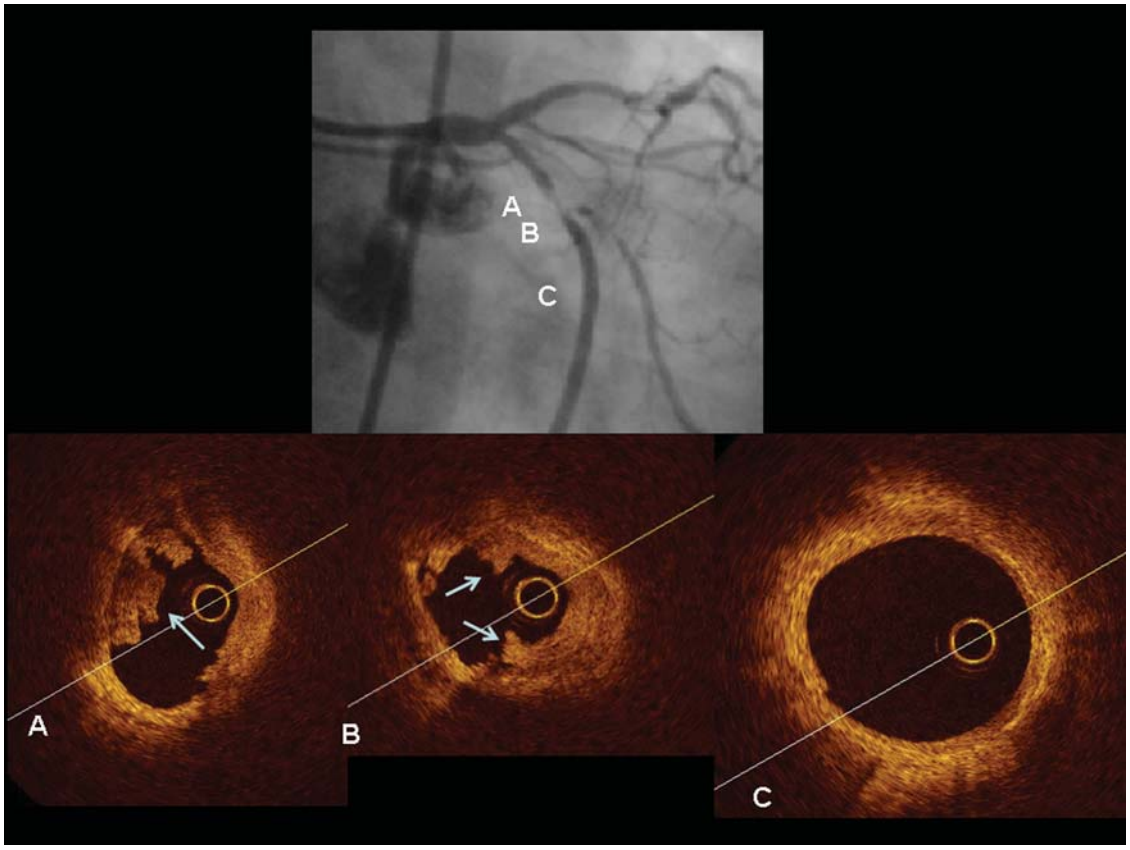

Figure 7 Culprit lesion in the left circumflex in a patient with unstable angina. Minimal dimensions of the optical coherence tomography probe enable an accurate visualization and quantification of lumen area (0.6 mm^2 in site B). Arrows show intracoronary thrombi at sites B and A, obtained 0.5 mm proximal to site B. In site C the proximal reference cross-section is displayed.

Measurements of atherosclerosis

Calibration

Accurate calibration is mandatory to fully realize the spatial resolution of OCT. The size of the OCT image is calibrated by adjusting the z-offset, the zero-point setting of the system. To maintain accurate measurements, the z-offset must be readjusted prior to offline analysis and monitored throughout the longitudinal segment. The tissue penetration of OCT rarely exceeds 1.0–1.3 mm. Therefore, in the presence of a large plaque burden, OCT fails to visualize the entire circumference of the IEL. Consequently, the plaque burden cannot be measured in the majority of target lesions. When measurable, the plaque is defined as the area between the inner lumen border and the media, delimited by the IEL. In these cases OCT measurements represent the 'true' histological area of the atheroma (or plaque) as opposed to the plaque and media typical of IVUS assessment. In fact, unlike IVUS, OCT can visualize the IEL and, therefore, can distinguish the atherosclerotic plaque from the muscular media.

As OCT depicts with high accuracy the interface between lumen and plaque, the definitions of 'lumen,' 'lesion stenosis,' and 'reference segment' are consistent with those currently applied for IVUS.

Stenosis. A stenosis is a lesion that compromises the lumen by at least 50% by cross-sectional area (CSA) compared with a predefined reference segment lumen.

Luminal area stenosis. The relative decrease in luminal area of the target lesion, in percent, when compared with a reference lumen area in the same vessel segment. The lumen area relative to the reference lumen area is analogous to the angiographic definition of diameter stenosis.

Minimal lumen area (MLA). Minimal lumen area along the length of the target lesion.

Maximum lumen diameter. The largest lumen diameter from one intimal leading edge to another along any line passing through the center of the lumen.

Minimum lumen diameter. The smallest lumen diameter from one intimal leading edge to another along any line passing through the center of the lumen.

Length of measurements. Lengths can be measured by the duration of the pullback and the pullback speed of the imaging fibre.

Proximal and distal reference lumen area. The site with the largest lumen either proximal or distal to a stenosis, but within the same segment (usually within 10 mm of the stenosis with no major intervening branches).

Optical coherence tomography can penetrate superficial *calcium deposits* unless their thicknesses exceed 1.0–1.5 mm. Therefore, the thicknesses of most superficial calcific formations can be determined. The arc of superficial calcium deposits can also be

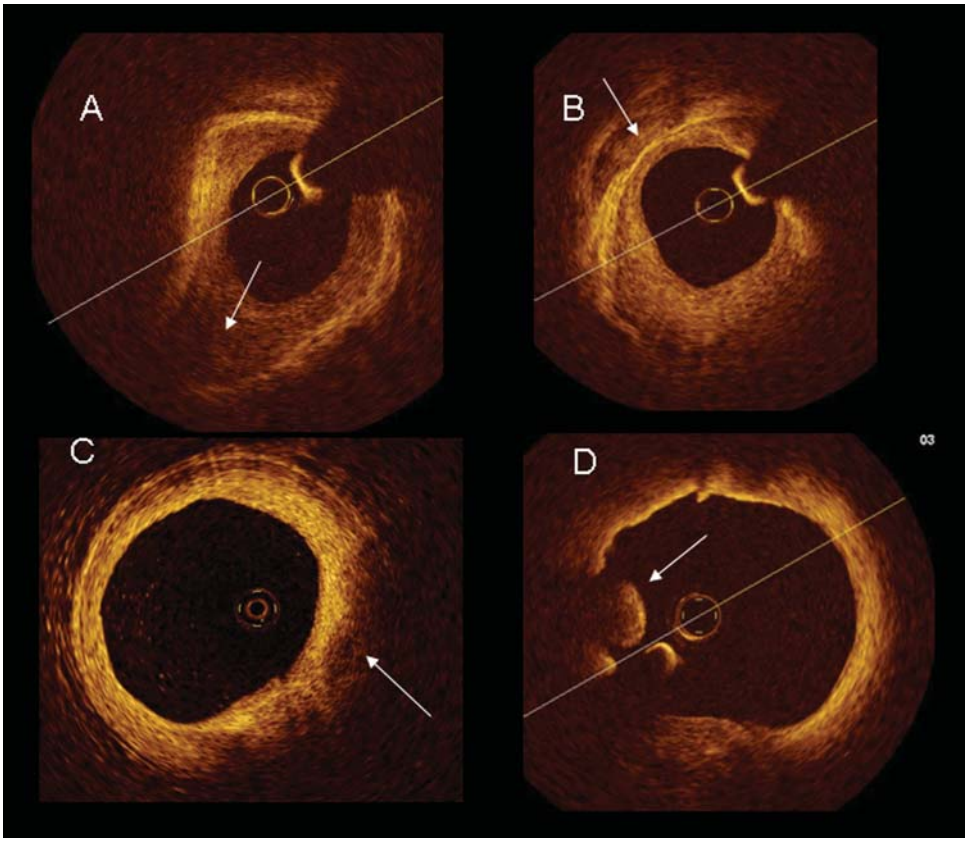

Figure 8 Optical coherence tomography penetration is due to plaque composition. Penetration is maximal for fibrotic tissue (*A*), and progressively less for calcific (*B*), lipid (*C*), and thrombus (*D*).

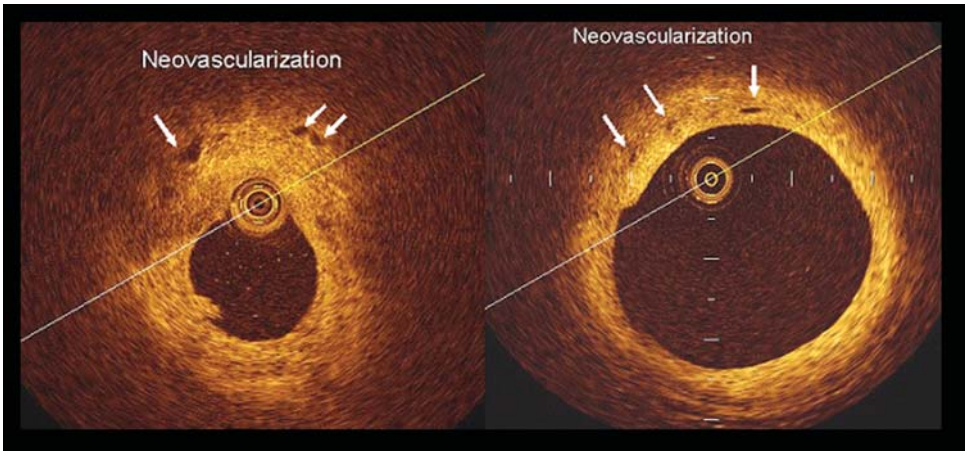

Figure 9 Presence of thin black holes at optical coherence tomography study, located in the outer plaque, near the adventitia (left panel) and in the inner plaque (right panel). These holes have a diameter of 50–100 μm and are likely due to plaque angioneogenesis.

measured (in degrees) with a protractor centred in the centre of the lumen.[10,11,22,23] By applying a semi-quantitative grading, calcium can be classified according to the number of quadrants it subtends (1, 2, 3, or 4). The length of the superficial calcific deposit can be measured using motorized transducer pull-back. Superficial micro-calcifications are small calcific deposits that subtend an angle less than 90 degrees and are separated from the lumen by a rim of tissue less than 100 μm thick.[10,11,22,23]

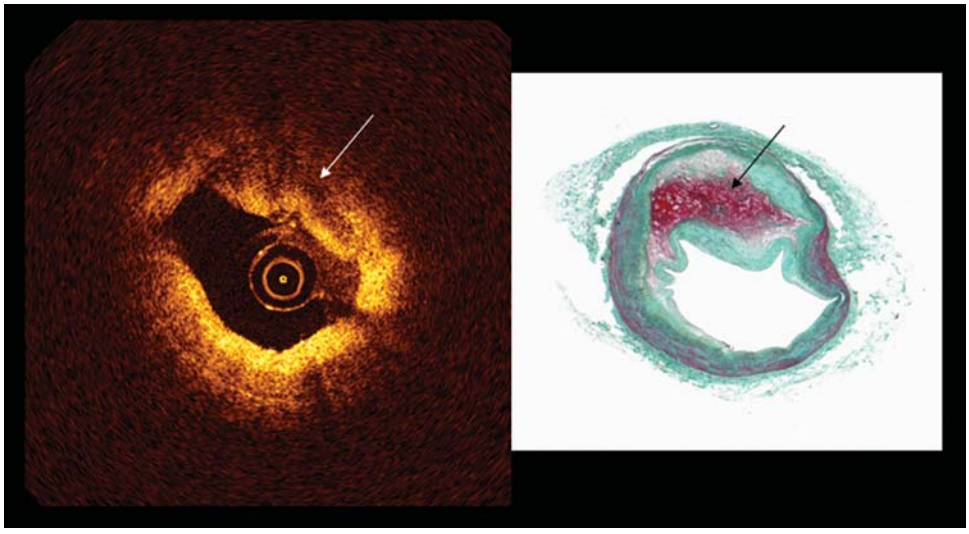

Figure 10 Optical coherence tomography detection of plaque haemorragy. The left panel shows a signal poor region (arrow) which corresponds to an haemorragic plaque region at histology (arrow in the right panel).

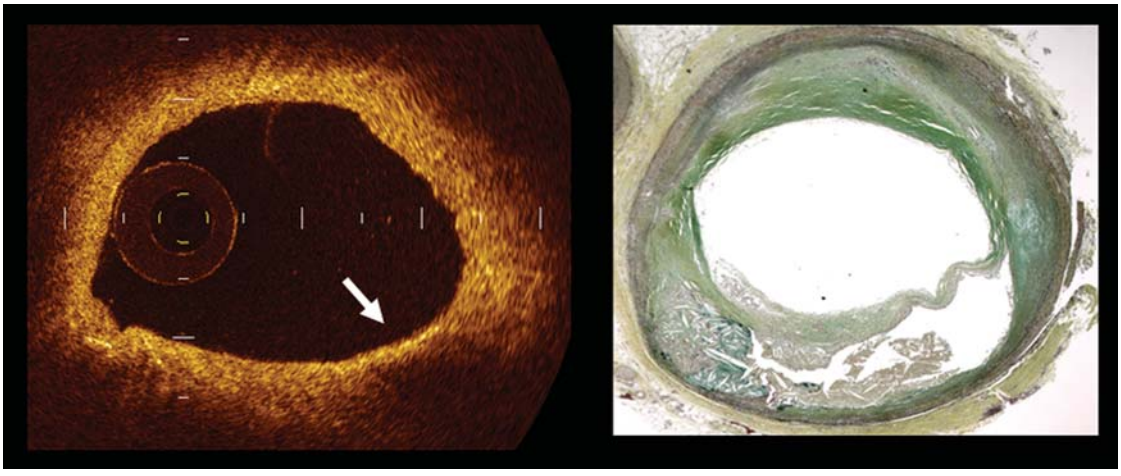

Figure 11 Left panel shows an optical coherence tomography example of cluster of foam cells, located in the fibrous cap and revealed as a band with high reflectivity (arrow). Right panel shows the corresponding histology.

Optical coherence tomography penetration through superficial *necrotic lipid pools* is less than that through calcified and fibrous tissues. Although the assessment of lipid-pool thickness would be an important piece of information, in the majority of lesions lipid pools thickness cannot be measured because of insufficient OCT imaging penetration.[10,11,21–24] However, the *thickness of the fibrous cap* delimiting superficial lipid pools can be measured by OCT. Fibrous-cap thickness can be obtained either as a single measurement at the cross-section where the fibrous cap thickness is considered minimal[27,28] or as the average of multiple (three or more) samples.[21,29] Further studies are needed to define an accurate methodology to assess fibrous cap thickness in humans and correlate these findings with clinical outcomes. Pathological studies of plaques leading to fatal events have established 65 μm as the threshold of fibrous cap thickness that best identifies thin, vulnerable lesions. This value can be adopted as a useful estimate for identifying thin caps prone to rupture *in vivo*. Optical coherence tomography has the image resolution to evaluate *in vivo* the validity of these concepts derived from post-mortem pathology studies. The thickness of the fibrous cap is not homogeneous throughout the plaque and its 3D longitudinal distribution should not be ignored. Semi-automated quantitative assessments will facilitate such evaluations.

The arc (in degrees) and the longitudinal extent of a superficial necrotic lipid pool can be measured as well. Furthermore, the size of a lipid necrotic pool can be graded semi-quantitatively according

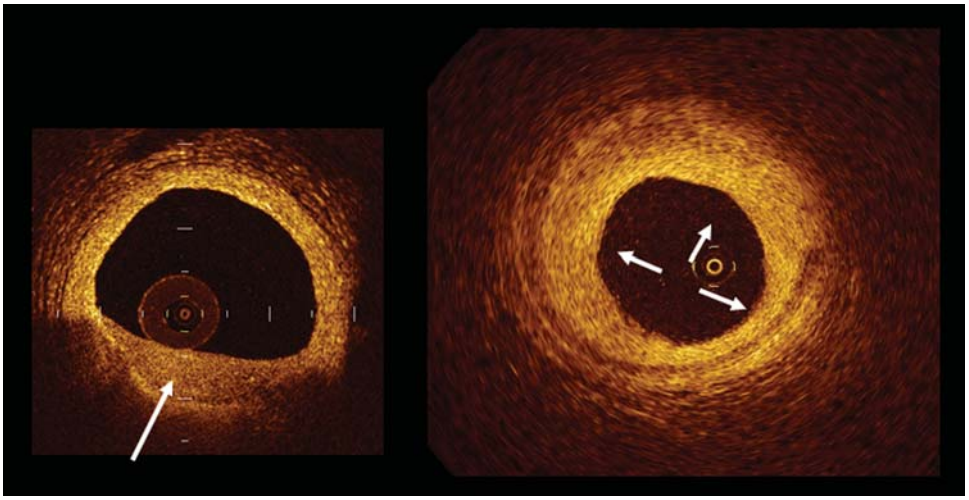

Figure 12 The figure shows that optical coherence tomography has the potential to identify loose fibrotic tissue (rich in proteoglycan) and dense (fibrotic) tissue. The left panel shows an example of loose connective tissue (arrow), which exhibits a lower reflectivity when compared with dense fibrotic tissue (right panel).

to the number of involved quadrants on the cross-sectional OCT images, and an estimate of the lipid content of a lesion can be derived from the number of quadrants occupied by necrotic lipid pool. By applying such semi-quantitative grading, necrotic lipid pools can be classified as absent or subtending 1, 2, 3, or 4 quadrants, analogous to the semi-quantitative grading of calcium.[11,23,29]

Controversial points in optical coherence tomography imaging of atherosclerosis

Identification of *erosion* as a mechanism of plaque instability is a challenge even for a technique with a resolution below 20 μm. Validation studies combining OCT with techniques providing a functional assessment of the endothelium may be able to give us more information on vessel thrombosis induced by erosion.

Optical coherence tomography has the potential to identify *angioneogenesis*. Despite the lack of specific validation studies, there is a general consensus that microvessels in plaque appear as thin black holes with a diameter of 50–100 μm that are present for at least 3–4 consecutive frames in pull-back images (*Figure 9*).

The identification of *plaque haemorrhage* and the link between plaque haemorrhage and plaque vulnerability are major issues that will require additional validation studies. Anecdotal observations indicate that haemorrhagic components appear as signal-poor OCT regions that must be distinguished from lipid necrotic pools. Further studies will be required to assess the ability of OCT to separate recent from old haemorrhagic areas and to clarify if haemosiderin can be distinguished from calcific components (*Figure 10*).

Optical coherence tomography has the potential to identify *inflammatory cells* such as clusters of lymphocytes. Streaks of foam cells are seen as bands of high reflectivity in OCT images. When macrophages are located in a plaque with a lipid pool, macrophage streaks appear within the fibrous cap covering the lipid pool. As already mentioned, the interface between the fibrous-cap and the lipid pool produces a bright OCT appearance that can be difficult to distinguish from tightly packed foam cells.[30,31]

Previous studies showed that application of OCT algorithm can identify inflammatory cells with high specificity and sensitivity. Offline use of this dedicated algorithm may be instrumental to identify and possibly quantify plaque inflammation. However it is felt that the applicability of these results to real-time imaging is questionable because the detection and quantification algorithms developed in these studies depend on accurate selection of the region of interest (*Figure 11*).

The types of *fibrous tissue* that can be identified by OCT need to be defined more specifically. Based on unpublished data OCT has the potential to distinguish loose fibrotic tissue (rich in proteoglycan) that has a low backscattering appearance with low signal attenuation from dense collagen tissue (*Figure 12*).

Current clinical applications: advantages and disadvantages of optical coherence tomography when compared with IVUS

Angiographically normal coronary arteries. Normal angiograms or angiograms with minimal irregularities are found in around 10–15% of patients undergoing coronary angiography for suspected coronary artery disease. Like IVUS, OCT can confirm the absence of significant atherosclerosis or indicate the degree of

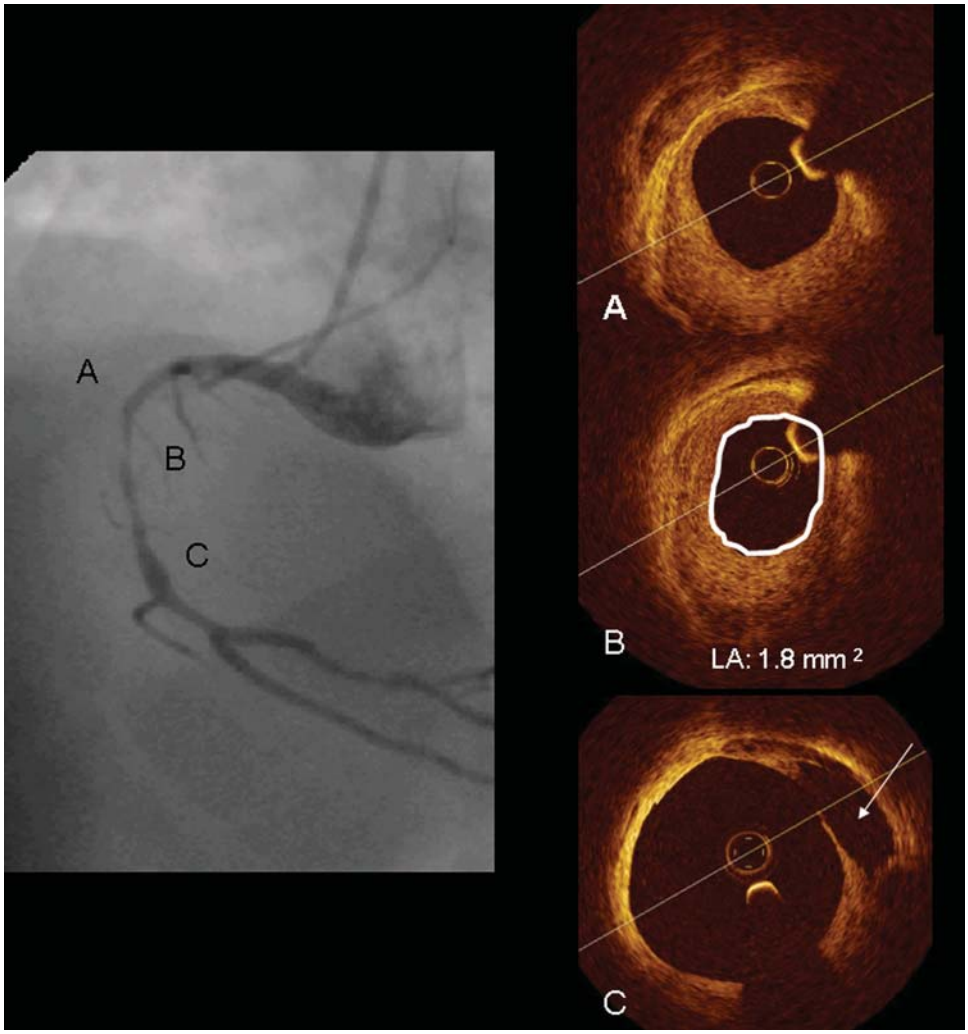

Figure 13 Example of stable severe lesion located in the right coronary artery. Optical coherence tomography shows a severe lumen narrowing with a lumen area (LA) that equals 1.8 mm^2. A stable plaque with a fibrous composition is present (*A* and *B*). Distal to the imaged lesion a previously ulcerated plaque, with a large cavity in contact with vessel lumen, is shown (arrow in *C*).

subclinical atherosclerotic lesion formation. This may have relevance to modulate the aggressiveness of medical therapeutic strategies for primary prevention.

Evaluation of intermediate stenoses and ambiguous lesions. Suboptimal angiographic visualization impairs the accurate assessment of stenosis severity. This may happen in the presence of intermediate lesions of uncertain severity, very short lesions, pre- or post-aneurysmal lesions, ostial or left main stem stenoses, disease at branching sites, sites with focal spasm, or angiographically hazy lesions. Optical coherence tomography has the potential to become a routine clinical tool to guide interventional procedures as it provides accurate luminal measurements of lesion severity due to a better delineation of the lumen–wall interface, when compared with IVUS.

However severity of plaques located at the very ostium of the left or right coronaries cannot be accurately addressed by OCT; in fact, at the current stage of technology, neither of the two OCT acquisition techniques (occlusive or non occlusive) appears to be suitable for aorto-ostial assessment.

Like IVUS, OCT can quantify lesion severity more accurately than quantitative coronary angiography, by measuring MLA, with 4 mm^2 being considered the significant cut-off threshold for a clinically significant flow-limiting stenosis in appropriately sized (>3 mm) vessels excluding the left main coronary artery (*Figure 13*). Further validation studies may be needed to corroborate this issue. Comparison of the MLA with reference lumen areas is an alternative method for assessment of the degree of stenosis.

In particular, OCT is indicated for assessment of angiographically hazy lesions and focal vessel spasm. The ability OCT to identify coronary thrombosis allows optimal assessment of lesion morphology in presence of haziness at angiography. Furthermore the relatively small size of OCT imaging catheters, compared with IVUS catheters, may reduce the incidence of catheter wedging and coronary spasm[15] (*Figure 14*).

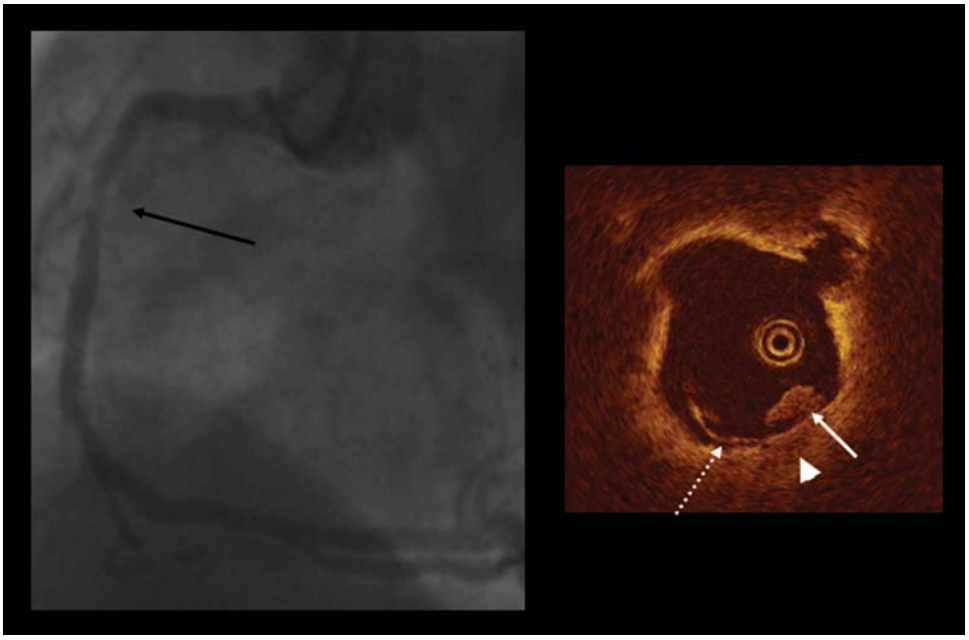

Figure 14 Identification of culprit lesion at the site of non-significant narrowing with angiographic haziness (*A*). Optical coherence tomography shows a mild dissection (dotted arrow) and thrombus (white arrow), facing a small lipid pool (arrow-head). A large portion of thrombus has been likely cleared by the adoption of anti-thrombotic treatment.

The main limitation of OCT resides in the inability to measure plaque burden whose thickness exceeds 1.3–1.5 mm. This drawback may affect the role of OCT in the setting of interventional procedures guidance, as well as overall disease severity.

Future clinical and research applications

Assessment of allograft vascular disease. Transplant allograft vascular disease (AVD) is characterized by diffuse fibrointimal proliferation with no pultaceous core and the absence of media remodelling. The intimal fibrous growth is typically concentric and diffuse as focal lesions are unusual in AVD. Coronary angiography underestimates the extension of the disease.[32] When compared with angiography, IVUS provides adjunctive information and is able to detect the fibrous intimal disease and the lack of remodelling. IVUS can also identify mural thrombi that are a frequent complication of AVD (over 75% of cases).[33] The clinical consequences of mural thrombi in AVD are largely underestimated in the clinical setting, being clinically silent in non-innervated hearts. Optical coherence tomography may become an appropriate imaging tool for monitoring the effects of preventive treatments in controlled studies.

Plaque vulnerability and its progression. IVUS currently plays an important role in the identification of plaque volume changes in response to specific treatments aimed at regression or cessation of progression.[34] OCT may prove to be an important addition to IVUS because it can discriminate among the different plaque components whose changes may be important in serial studies. However robust validation studies are needed to verify whether OCT is capable of measuring serial changes in plaque components indicative of vulnerability such as fibrous cap thickness or lipid pool extension.

Due to its ability to address plaque components related to vulnerability, OCT may have a role for assessing the risk of myocardial infarction. This clinical application, however, needs to be proven in the future.

Future optical coherence tomography developments

Currently, standard OCT interpretation is limited to the evaluation of grey-scale images generated by infra-red light reflections at tissue interfaces. The high resolution of OCT when compared with IVUS enables the identification of the main plaque components that include lipid pools, calcium, fibrotic tissue, and thrombus. However, identification of individual plaque components by OCT requires experience; for instance, in order to distinguish calcium from lipids, a careful analysis of optical properties of the plaque components must be done. Furthermore, use of grey-scale images seems more suited for the assessment of the overall composition of homogeneous plaques while heterogeneous plaque regions (often constituted of adjacent areas of micro-calcifications and lipid) are more common in vulnerable plaques. The application of a post-processing colour-coding software-based algorithm on analysis of either spectral OCT backscattered data or other optical tissue properties should improve the characterization of atherosclerotic coronary plaques and provide a more objective assessment.[35]

Three-dimensional reconstruction of OCT-analysed vessel segments promises to improve our understanding of vessel and plaque pathology and may facilitate histopathologic OCT studies

by providing a true view of coronary architecture. The localization and quantitative analysis of elements related to plaque instability—such as the lipid necrotic core, fibrous cap, or plaque angiogenesis—are likely to be improved by multi-dimensional analysis. Also, OCT identification of plaque cellular components, such as inflammatory cells, is likely to be improved by 3D visualization.[36,37] The recent introduction of fast Fourier-domain OCT imaging may facilitate the acquisition of 3D data from pull-back image sequences.

Funding

This study was not funded or granted by medical association, professional society, or private industry.

Conflict of interest: none declared.

References

1. Huang D, Swanson EA, Lin CP, Schuman JS, Stinson WG, Chang W, Hee MR, Flotte T, Gregory K, Puliafito CA. Optical coherence tomography. *Science* 1991; **254**:1178–1181.
2. Brezinski ME, Tearney GJ, Bouma BE, Izatt JA, Hee MR, Swanson EA, Southern JF, Fujimoto GJ. Optical coherence tomography for optical biopsy properties and demonstration of vascular pathology. *Circulation* 1996;**93**:1206–1213.
3. Rogowska J, Patel NA, Fujimoto JG, Brezinski ME. Optical coherence tomographic elastography technique for measuring deformation and strain of atherosclerotic tissues. *Heart* 2004;**90**:556–562.
4. Fujimoto JG, Schmitt JM. Principles of OCT. In: van Leeuwen TG, Serruys P, eds. *Handbook of Optical Coherence Tomography in Cardiovascular Research*. Abingdon, UK: Taylor & Francis; 2006. p19–33.
5. Kawase Y, Hoshino K, Yoneyama R, McGregor J, Hajjar RJ, Jang IK, Hayase M. In vivo volumetric analysis of coronary stent using optical coherence tomography with a novel balloon occlusion-flushing catheter: a comparison with intravascular ultrasound. *Ultrasound Med Biol* 2005;**31**:1343–1349.
6. Yun SH, Tearney GJ, Vakoc BJ, Shishkov M, Oh WY, Desjardins AE, Suter MJ, Chan RC, Evans JA, Jang IK, Nishioka NS, de Boer JF, Bouma BE. Comprehensive volumetric optical microscopy in vivo. *Nat Med* 2006;**12**:1429–1433.
7. Schmitt JM, Huber R, Fujimoto JG. Limiting ischemia by fast Fourier-domain imaging. In: Regar E, van Leeuwen TG, Serruys PW, eds. *Optical Coherence Tomography in Cardiovascular Research*. London: Informa Healthcare; 2007.
8. Peterson CL, Schmitt JM. Design of an OCT imaging system for intravascular applications. In: van Leeuwen TG, Serruys P eds., *Handbook of Optical Coherence Tomography in Cardiovascular Research*. Abingdon, UK: Taylor & Francis; 2006. p35–42.
9. Swanson EA, Peterson CL. Methods and apparatus for high speed longitudinal scanning in imaging systems. *United States Patent* 2001;**191**:862.
10. Yabushita H, Bouma BE, Houser SL, Aretz HT, Jang IK, Schlendorf KH, Kauffman CR, Shishkov M, Kang DH, Halpern EF, Tearney GJ. Characterization of human atherosclerosis by optical coherence tomography. *Circulation* 2002; **106**:1640–1645.
11. Jang IK, Bouma BE, Kang DH, Park SJ, Park SW, Seung KB, Choi KB, Shishkov M, Schlendorf K, Pomerantsev E, Houser SL, Aretz T, Tearney GJ. Visualization of coronary atherosclerotic plaques in patients using Optical Coherence Tomography: comparison with intravascular ultrasound. *J Am Coll Cardiol* 2002;**39**: 604–609.
12. Regar E, Prati F, Serruys PW. Intracoronary OCT application: methodological considerations. In: van Leeuwen TG, Serruys P, eds. *Handbook of Optical Coherence Tomography*. Abingdon, UK: Taylor & Francis; 2006. p53–64.
13. Tanigawa J, Barlis P, Di Mario C. Intravascular optical coherence tomography: optimisation of image acquisition and quantitative assessment of stent strut apposition. *EuroInterv* 2007;**3**:128–136.
14. Prati F, Cera M, Ramazzotti V, Imola F, Giudice R, Giudice M, De Propris S, Albertucci M. From bench to bed side: a novel technique to acquire OCT images. *Circ J* 2008;**72**:839–843.
15. Prati F, Cera M, Ramazzotti V, Imola F, Giudice R, Albertucci M. Safety and feasibility of a new non-occlusive technique for facilitated intracoronary optical coherence tomography (OCT) acquisition in various clinical and anatomical scenarios. *EuroInterv* 2007;**3**:365–370.
16. Yamaguvhi T, Terashima M, Akasaka T, Hayashi T, Mizuno K, Muramatsu T, Nakamura M, Nakamura S, Saito S, Takano M, Takayama T, Yoshikawa J, Suzuki T. Safety and feasibility of an intravascular optical coherence tomography image wire system in the clinical setting. *Am J Cardiol* 2008;**101**:562–567.
17. Kawasaki M, Bouma BE, Bressner J, Houser SL, Nadkarni SK, MacNeill BD, Jang IK, Fujiwara H, Tearney GJ. Diagnostic accuracy of optical coherence tomography and integrated backscatter intravascular ultrasound images for tissue characterization of human coronary plaques. *J Am Coll Cardiol* 2006;**48**:81–88.
18. Kume T, Akasaka T, Kawamoto T, Watanabe N, Toyota E, Neishi Y, Sukmawan R, Sadahira Y, Yoshida K. Assessment of coronary intima-media thickness by Optical Coherence Tomography. Comparison with intravascular ultrasound. *Circ J* 2005;**8**: 903–907.
19. Di Mario C, Görge G, Peters R, Kearney P, Pinto F, Hausmann D, von Birgelen C, Colombo A, Mudra H, Roelandt J, Erbel R, on behalf of the Study Group on Intracoronary Imaging of the Working Group of Coronary Circulation of the Subgroup on Intravascular Ultrasound of the Working Group of Echocardiography of the European Society of Cardiology. Clinical application and image interpretation in intracoronary ultrasound. *Eur Heart J* 1998;**19**:207–229.
20. Mintz GS, Nissen SE, Anderson WD, Bailey SR, Erbel R, Fitzgerald PJ, Pinto FJ, Rosenfield K, Siegel RJ, Murat Tuzcu E, Yock PG, O'Rourke RA, Abrams J, Bates ER, Brodie BR, Douglas PS, Gregoratos G, Hlatky MA, Hochman GS, Kaul S, Tracy CM, Waters DD, Winters WL. ACC Clinical Expert Consensus Document on Standards for the acquisition, measurement and reporting of intravascular ultrasound studies: a report of the American College of Cardiology Task Force on Clinical Expert Consensus Documents (Committee to Develop a Clinical Expert Consensus Document on Standards for Acquisition, Measurement and Reporting of Intravascular Ultrasound Studies [IVUS]. *J Am Coll Cardiol* 2001; **37**:1478–1492.
21. Kubo T, Imanishi T, Takarada S, Kuroi A, Ueno S, Yamano T, Tanimoto T, Matsuo Y, Masho T, Kitabata H, Tsuda K, Tomobuchi Y, Akasaka T. Assessment of culprit lesion morphology in acute myocardial infarction: ability of Optical Coherence Tomography compared with intravascular ultrasound and coronary angioscopy. *J Am Coll Cardiol* 2007;**50**:933–939.
22. Jang IK, Tearney GJ, MacNeill B, Takano M, Moselewski F, Iftima N, Shishkov M, Houser S, Aretz HT, Halpern EF, Bouma BE. In vivo characterization of coronary atherosclerotic plaque by use of Optical Coherence Tomography. *Circulation* 2005;**111**:1551–1555.
23. Kume T, Akasaka T, Kawamoto T, Watanabe N, Toyota E, Neishi Y, Sukmawan R, Sadahira Y, Yoshida K. Assessment of coronary arterial plaque by Optical Coherence Tomography. *Am J Cardiol* 2006;**97**:1172–1175.
24. Zimarino M, Prati F, Stabile E, Pizzicannella J, Fouad T, Filippini A, Rabozzi R, Trubiani O, Pizzicannella G, De Caterina R. Optical coherence tomography accurately identifies intermediate atherosclerosis lesions. An in-vivo evaluation in the rabbit carotid artery. *Atherosclerosis* 2007;**193**:94–101.
25. Kume T, Akasaka T, Kawamoto T, Ogasawara Y, Watanabe N, Toyota E, Neishi Y, Sukmawan R, Sadahira Y, Yoshida K. Assessment of coronary arterial thrombus by Optical Coherence Tomography. *Am J Cardiol* 2006;**97**:1713–1717.
26. Takano M, Jang IK, Inami S, Yamamoto M, Murakami D, Okamatsu K, Seimiya K, Ohba T, Mizuno K. In vivo comparison of optical coherence tomography and angioscopy for the evaluation of coronary plaque characteristics. *Am J Cardiol* 2008;**101**:471–478.
27. Kume T, Akasaka T, Kawamoto T, Okura H, Watanabe N, Toyota E, Neishi Y, Sukmawan R, Sadahira Y, Yoshida K. Measurements of the thickness of the fibrous cap by optical coherence tomography. *Am Heart J* 2006;**152**:755.e1–755.e4.
28. Barlis P, Serruys PW, Gonzalo N, van der Giessen WJ, de Jaegere PJ, Regar E. Assessment of culprit and remote coronary narrowings using optical coherence tomography with long-term outcomes. *Am J Cardiol* 2008;**102**:391–395.
29. Raffel OC, Merchant FM, Tearney GJ, Chia S, DeJoseph Gauthier D, Pomerantsev E, Mizuno K, Bouma BE, Jang IK. In vivo association between positive coronary artery remodelling and coronary plaque characteristics assessed by intravascular optical coherence tomography. *Eur Heart J* 2008;**29**:1721–1728.
30. Tearney GJ, Yabushita H, Houser SL, Aretz HT, Jang IK, Schlendorf KH, Kauffman CR, Shishkov M, Halpern EF, Bouma BE. Quantification of macrophage content in atherosclerotic plaques by optical coherence tomography. *Circulation* 2003;**107**:113–119.
31. Raffel OC, Tearney GJ, Gauthier DD, Halpern EF, Bouma BE, Jang IK. Relationship between a systemic inflammatory marker, plaque inflammation, and plaque characteristics determined by intravascular optical coherence tomography. *Arterioscler Thromb Vasc Biol* 2007;**27**:1820–1827.
32. St Goar FG, Pinto FJ, Alderman EL, Valentin HA, Schroeder JS, Gao S, Stinson EB, Popp RL. Intracoronary ultrasound in cardiac transplant recipients: in vivo evidence of angiographically silent intimal thickening. *Circulation* 1992;**85**:979–987.
33. Hunt SA, Bristow MR, Kubo SH, O'Connell JB, Young JB. Guidelines for training in adult cardiovascular medicine. Core Cardiology Training Symposium (COCATS). Task Force 8: training in heart failure and transplantation. *J Am Coll Cardiol* 1995; **25**:29–31.
34. Nicholls SJ, Tuzcu EM, Sipahi I, Grasso AW, Schoenhagen P, Hu T, Wolski K, Crowe T, Desai MY, Hazen SL, Kapadia SR, Nissen SE. Statins, high-density

lipoprotein cholesterol, and regression of coronary atherosclerosis. *JAMA* 2007; **297**:499–508.
35. Nair A, Kuban BD, Tuzcu EM, Schoenhagen P, Nissen SE, Geoffrey Vince D. Coronary plaque classification with intravascular ultrasound radiofrequency data analysis. *Circulation* 2002;**106**:2200–2206.
36. Von Birgelen C, de Vrey EA, Mints GS, Nicosia A, Bruining N, Li W, Slager CJ, Roelandt JRTC, Serruys PW, de Feyter PJ. ECG-gated three-dimensional intravascular ultrasound: feasibility and reproducibility of the automated analysis of coronary lumen and atherosclerotic plaque dimensions in humans. *Circulation* 1997;**96**:2944–2952.
37. Slager CJ, Wentzel JJ, Schuurbiers JC, Oomen JAF, Kloet J, Krams R, von Birgelen C, van der Giessen WJ, Serruys PW, de Feyter PJ. True 3-dimensional reconstruction of coronary arteries in patients by fusion of angiography and IVUS (ANGUS) and its quantitative validation. *Circulation* 2000;**102**:511–516.

CARDIOVASCULAR FLASHLIGHT

doi:10.1093/eurheartj/ehp511
Online publish-ahead-of-print 3 December 2009

Three-dimensional reconstruction imaging of the human foetal heart in the first trimester

Hikoro Matsui[1], Timothy Mohun[2], and Helena M. Gardiner[1]*

[1]Institute of Reproductive and Developmental Biology, Faculty of Medicine, Imperial College, Queen Charlotte's and Chelsea Hospital, Du Cane Road, London W12 0HS, UK and [2]Division of Developmental Biology, MRC National Institute of Medical Research, London, UK

* Corresponding author. Tel: +44 207 351 8719, Fax: +44 207 351 8129, Email: helena.gardiner@imperial.ac.uk

High-resolution episcopic microscopy (HREM) is a novel method producing high-quality, three-dimensional (3D) images of tissue from a variety of species. We report, for the first time, the use of HREM to create high-resolution 3D reconstructions of the human foetal heart in the first trimester. These models are suitable for a detailed morphological investigation to produce 'virtual' images of any section plane and 3D models that can be examined using 'virtual' dissection.

Following ethical approval by our institutional review committee and written consents, we collected normal foetal hearts from surgical termination of singleton pregnancies followed by HREM processing, including automatic image capturing of the surface of sectioned sample blocks. Each captured image data set was used to generate 3D models by volume rendering.

The detailed structures can be seen more clearly in the HREM reconstruction (*Panel B*) than in the original photograph (*Panel A*). In this normal 11-week heart (modelled with an isotropic resolution of 3 μm), we can clearly observe several specific features of the human foetal heart, including large atrial appendages, prominent coronary arteries, and the relatively small size of the atrial chambers (*Panels B* and *F*). Volume rendering, which allows internal morphology of the heart to be examined at high resolution, shows thickened great arterial walls (*Panels C–E*) and details of valve and septal architecture (*Panels C* and *D*). Multi-planar reconstructed images demonstrate detailed structures of the inside of cardiac chambers (*Panels E* and *F*).

The HREM is a useful tool to investigate the morphology of the human foetal heart in early gestation when manual manipulation is difficult and has the potential to act as a gold-standard of normal and abnormal foetal cardiac morphology to inform 3D foetal echocardiographical studies.

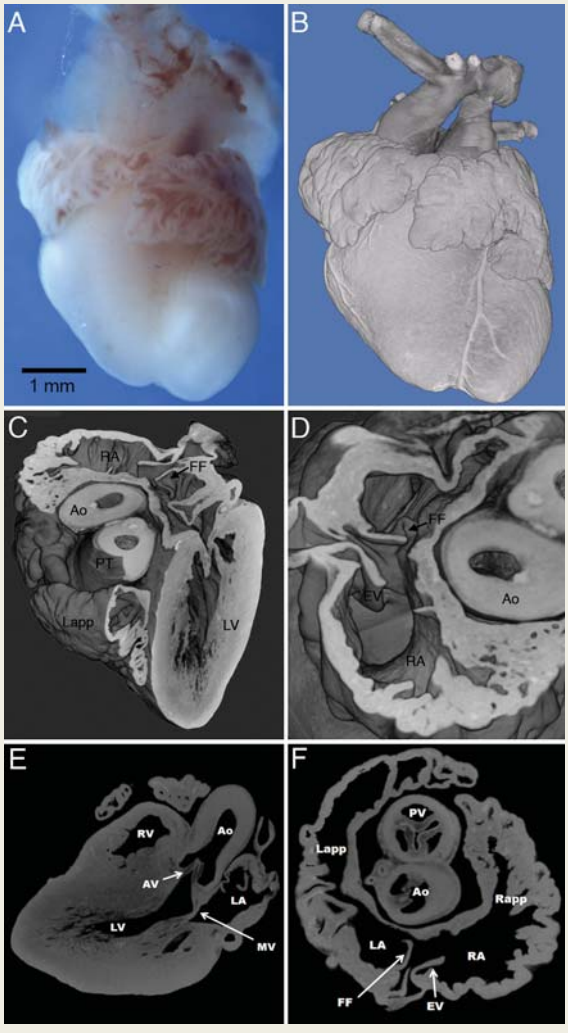

Abbreviations used in the figures are: Ao, aorta; AV, aortic valve; EV, Eustachian valve; FF, foramen flap; LA, left atrium; Lapp, left atrial appendage; LV, left ventricle; MV, mitral valve; PT, pulmonary trunk; PV, pulmonary valve; RA, right atrium; Rapp, right atrial appendage.

H.M. is supported by TinyTickers, the foetal heart charity (www.tinytickers.org). H.M. and H.G. are grateful for support from the NIHR Biomedical Research Centre funding scheme.